Electromagnetics
Publication details, including instructions for authors and subscription information:
http://www.informaworld.com/smpp/title~content=t713770615

TE EXCITATION OF AN UNCLOSED CIRCULAR CYLINDER AT THE PLANAR PENETRABLE INTERFACE

Natasha V. Veremey [a]; Alexander I. Nosich [a]; Vladimir V. Veremey [a]
[a] Institute of Radiophysics and Electronics of the Academy of Sciences of Ukraine. Kharkov. Ukraine

To cite this Article: Natasha V. Veremey, Alexander I. Nosich and Vladimir V. Veremey , 'TE EXCITATION OF AN UNCLOSED CIRCULAR CYLINDER AT THE PLANAR PENETRABLE INTERFACE', Electromagnetics, 13:2, 169 - 186
To link to this article: DOI: 10.1080/02726349308908341
URL: http://dx.doi.org/10.1080/02726349308908341

TE EXCITATION OF AN UNCLOSED CIRCULAR CYLINDER AT THE PLANAR PENETRABLE INTERFACE

Natasha V. Veremey, Alexander I. Nosich, and
Vladimir V. Veremey
Institute of Radiophysics and Electronics
of the Academy of Sciences of Ukraine
12, Acad. Proskura str., Kharkov, 310085, Ukraine

ABSTRACT.

An analysis of two-dimensional scattering from an unclosed circular cylinder in the vicinity of the plane penetrable interface between two semi-infinite homogeneous half spaces of the same or of different electromagnetic properties is presented. The perfectly conducting axially slotted cylinder is of infinite extent and the excitation is transverse electric to the cylinder axis.

The final infinite system of linear algebraic equations for expansion coefficients of the current density function is obtained from the dual series equations by the method of Riemann-Hilbert Problem. The system may be solved by truncation of an infinite matrix with further usage of ordinary inversion methods. The cylinder is excited by a plane wave or by a line magnetic-current source. Some data displaying the frequency dependencies of the scattering cross-section and radiation resistance, as well as the far-field patterns, are presented and discussed.

INTRODUCTION

An analysis of the scattering from a perfectly electrically conducting unclosed circular cylinder (screen), i.e., the cylinder with a longitudinal slot, in the vicinity of the penetrable planar interface between two half-spaces of similar of dissimilar electromagnetic properties is presented. Cross-section views of the screen, half-spaces and a penetrable surface of interest are depicted in Fig.1.

The plane penetrable surface is characterized by complex reflection and transmission coefficients R and T. The upper half-space ($y > 0$) is denoted as the region

Electromagnetics 13:169–186, 1993

0272-6343/93 $10.00 + .00

S_1 and is characterized by ε_1 while the lower half-space ($y < -b$) is denoted as the region S_2 and is characterized by ε_2. The unclosed screen may be located either above or below the interface between the two half-spaces, not interesting with it. The slot width and its orientation angle are taken arbitrarily. The structure is excited by a plane wave with the vector H parallel to the axis of the cylinder, or by line magnetic current (line dipole). Thus the whole problem is a two-dimensional one. The excitation depends upon the time according to $e^{-i\omega t}$, which term is suppressed.

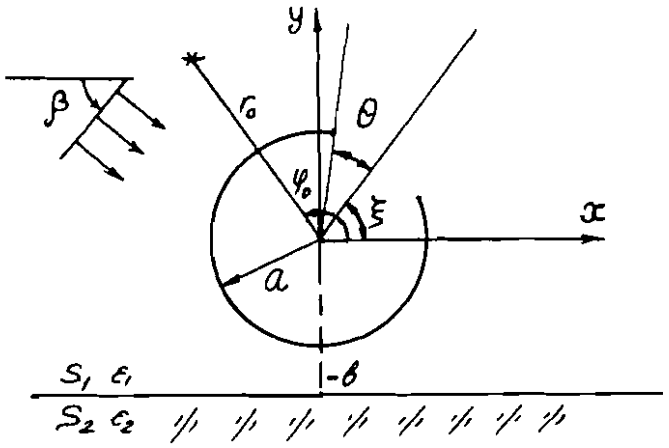

Fig.1 Circular unclosed cylinder located near the interface between two semi-infinite half-space and illuminated by plane wave or by magnetic-current source in the upper half-space.

There exist a number of papers treating the problems of TM or TE wave scattering by a conducting cylinder of a general cross-section located near the plane interface, e.g., by a buried cylinder. In [1,2] some very interesting numerical results have been obtained for circular and rectangular cylinders and strips parallel and perpendicular to the interface between two dielectric media. As for thin screens, the analysis of free-space TM or TE excitation has been presented in [3,4]. It has been shown that a TE-excited unclosed circular cylinder has sharp resonant properties, even in the low-frequency range, due to the excitation of the so-called Helmholtz natural mode of an open cavity.

The paper presented treats the case of a TE-excited unclosed screen located

near either a plane penetrable surface or a plane boundary of two different media. In comparison with simple scatterers treated in [1,2], such a cylinder has pronounced resonant features. Besides, for the line current excitation, the screen may serve as an antenna reflector. That is why the geometry considered in this paper models at least two situations of practical interest: an open resonator with a penetrable plane mirror (e.g., shortperiodic diffraction grating), and a reflector antenna near a flat boundary (e.g., that of the Earth).

Integral representation of the scattered field is obtained by using the 2-D Green's function of the space containing a flat interface. By expansion into angular Fourier series, the problem considered is reduced at first to dual series equation for expansion coefficients of the current density on the screen. The system of linear algebraic equations is obtained by inverting the static part of the equations operator. This system may be solved by truncation of the infinite matrix with further usage some of ordinary inversion methods.

The numerical treatment results in the calculation of the frequency dependencies of the screen's total scattering cross-sections of the screen radiation resistance (for the line current excitation). Besides, the far-field patterns of the reflector antenna are presented, both for "buried" and "elevated" antenna geometries.

FORMULATION OF THE PROBLEM

Assume an incident TE-wave $H^0(\vec{r})$ to excite the screen in the presence of the plane interface given in Fig.1. The exact form of $H^0(\vec{r})$ depends on the type of the source. We shall consider two cases: plane wave and line magnetic current excitation; the corresponding explicit formulae for the incident fields may be found in Appendix 1.

The total fields is the sum of incident and induced ones

$$H(\vec{r}) = H^0(\vec{r}) + H^{sc}(\vec{r}) \tag{1}$$

The scattered field satisfies the Helmholtz equation

$$(\Delta + k_j^2)H^{sc}(\vec{r}) = 0 \tag{2}$$

where $k_j = k\varepsilon_j^2$, $k = \omega/c$, $\varepsilon_j (j = 1, 2)$ are the corresponding dielectric constants of upper and lower half-spaces, $\vec{r} \in R^2 \backslash (\partial M, y = -b)$, ∂M is the cross-sectional contour of the screen. The boundary conditions on the interface and the screen are, respectively

$$\hat{B} H(\vec{r})\Big|_{y=-b} = 0, \tag{3}$$

and

$$\frac{\partial}{\partial n} H(\vec{r})\Big|_{\vec{r} \in \partial M} = 0, \tag{4}$$

where exact form of operator $\hat{B}$ depends on the type of the boundary. E.g., for plane dielectric interface we have

$$\begin{gathered} H(x, -b+0) - H(x, -b-0) = 0 \\ \frac{\partial}{\varepsilon_1 \partial y} H(x, -b+0) - \frac{\partial}{\varepsilon_2 \partial y} H(x, -b-0) = 0 \end{gathered} \tag{3'}$$

Besides, because of sharp edges of the screen, we have to use the so-called edge condition ensuring that

$$\int\limits_{S \subset R^2} \left(k^2 \varepsilon |H|^2 + |\nabla H|^2\right) d\vec{r} < \infty \tag{5}$$

for any compact region S containing the edge.

Finally, to complete the formulation of the problem, we have to introduce some kind of condition at infinity ($r \to \infty$). This is a somewhat specific point for the whole treatment, as the geometry of the problem contains the infinite boundary $y = -b$ beside the finite boundary of the scatterer ∂M. If there are no losses ($\operatorname{Im} \varepsilon_{1,2} = 0$), then the well-known Sommerfeld radiation condition is not always valid. Thorough investigation of this question [5] shows that a more general radiation condition takes place

$$H_j^{sc}(\vec{r}) \underset{r \to \infty}{\sim} \Psi_j^{sc}(\varphi) \frac{e^{ik_j r}}{(0.5 i \pi k_j r)^{1/2}} + \sum_{q=1}^{Q} a_q V_q(y) e^{ih_q \gamma_q |x|}, \tag{6}$$

where $V_q(y)$ are the natural surface (unattenuating) modes of the interface propagating with wavenumbers $h_q : \min\limits_j k_j < h < \max\limits_j k_j$, $\gamma_q = \operatorname{sign} dh_q(k)/dk$, Q is the number of modes, $j = 1, 2$. For some simple types of boundaries, such as dielectric interface and plane grating of perfectly conducting strips, there are no

natural surface modes of the boundary. Then (6) is reduced to the Sommerfeld radiation condition.

DERIVATION OF BASIC EQUATIONS.

It is not difficult to show that the scattered field may be represented by potential-type integral (a double-layer one due to the TE character of the field)

$$H^{sc}(\vec{r}) = \int\limits_{\partial M} \mu(\vec{r}) \frac{\partial}{\partial n'} G(\vec{r}, \vec{r}\,')dr', \tag{7}$$

where function $\mu(\vec{r}\,')$ is the density of the current induced on the screen, while $G(\vec{r}, \vec{r}\,')$ is the Green's function of the 2-D space with a flat penetrable boundary specified by means of the boundary operator $\hat{B}$. $G(\vec{r}, \vec{r}\,')$ has to satisfy the problem which is very similar to the above described one but without conditions (4) and (5) associated with the compact scatterer.

From the most general point of view, this function may be presented as the sum of singular and regular parts

$$G(\vec{r}, \vec{r}\,') = \frac{i}{4}\delta_{1j} H_0^{(1)}(k_1|\vec{r} - \vec{r}\,'|) + G_j^{sc}(\vec{r}, \vec{r}\,') \tag{8}$$

where $\vec{r} \in S_1$, $\vec{r} \in S_j (j = 1, 2)$

The secondary part of the Green's function may be treated as a Fourier-type integral

$$G_j^{sc}(\vec{r}, \vec{r}\,') = \frac{i}{4\pi} \int\limits_{-\infty}^{\infty} \frac{e^{ig_1 b}}{g_j} \begin{Bmatrix} R(h)e^{ig_1(y+y')}, & j = 1 \\ T(h)e^{-ig_2(y-y')}, & j = 2 \end{Bmatrix} e^{ih(x-x')} dh, \tag{9}$$

where $g_j = (k_j^2 - h^2)^{1/2}$, and the quantities of $R(h)$ and $T(h)$ are the reflection and transmission coefficients of the plane penetrable interface.

Substituting integral (7) into boundary condition (4) we obtain the integral-differential equation

$$\frac{\partial}{\partial n} \int\limits_{\partial M} \mu(\vec{r}) \frac{\partial}{\partial n'} G(\vec{r}, \vec{r}\,')dr' \Big|_{\vec{r} \in \partial M} = -\frac{\partial H^0}{\partial n}\Big|_{\vec{r} \in \partial M} \tag{10}$$

which can be solved numerically. But this approach is noteffective.

In our case the circular shape of the screen suggest a simple way of discretizing the problem. Let us expand all the quantities into the Fourier series over angular functions, namely

$$\mu(\vec{r}\,') = \frac{i}{2\pi k_1 a} \sum_{(n)} \mu_n e^{in\varphi'}, \tag{11}$$

$$\left.\frac{\partial H^0(\vec{r})}{\partial n}\right|_{\vec{r}\in\partial M} = \sum_{(n)} f'_n e^{in\varphi}, \tag{12}$$

where the explicit form of f'_n coefficients depends on the type of the excitation (see Appendix 1), while the coefficients μ_n are unknowns to be sought for.

As for the Green's function $G(\vec{r},\vec{r}\,')$, we obtain in a similar way for $\vec{r}\,' \in S_1$, $\vec{r} \in S_j$,

$$G_j^{sc}(\vec{r},\vec{r}\,') = \sum_{(n)}\sum_{(p)} J_{-n}(k_1 r') J_p(k_j r) \Omega^j_{n+p} e^{ip\varphi - in\varphi'},$$

where

$$\Omega^j_n = \frac{i^{n+1}}{4\pi} \int_{-\infty}^{\infty} \frac{e^{in\psi_j}}{g_j} \begin{Bmatrix} R(h)e^{i2g_1 b}, & j=1 \\ T(h), & j=2 \end{Bmatrix} dh \tag{13}$$

and $\cos\psi_j = h/k_j$, $\sin\psi_j = -g_j/k_j = -(1-h^2/k_j^2)^{1/2}$.

Taking into account these series, we can integrate in (10) and make a term by term differentiation (assuming it is valid), which results in the dual series equations

$$\sum_{(n)} \mu_n \left[J'_n(k_1 a) H_n^{(1)'}(k_1 a) + J_{-n}(k_1 a) \sum_{(p)} J'_p(k_1 a) \Omega^1_{n+p} e^{ip\varphi} \right] =$$
$$-\sum_{(n)} f'_n e^{in\varphi}, \qquad \theta < |\varphi - \xi| \le \pi,$$
$$\sum_{(n)} \mu_n e^{in\varphi} = 0, \qquad |\varphi - \xi| < \theta \tag{14}$$

Besides, edge condition (5) produces the following inequality in terms of current coefficients

$$\sum_{(n)} |\mu_n|^2 |n+1| < \infty \tag{15}$$

Equations (14) have canonical form to be regularized by means of the Riemann-Hilbert Problem technique (see[6] for details). The final system of linear algebraic equations is as follows

$$\mu_m = \sum_{(n)} A_{mn}\mu_n + B_m, \qquad m = 0, \pm 1, \ldots \tag{16}$$

where

$$A_{mn} = \Delta_n T_{mn} + i\pi(k_1 a)^2 J'_{-n}(k_1 a) \sum_{(p)} J'_p(k_1 a)\Omega^1_{n+p} T_{mp}$$

$$B_m = i\pi(k_1 a)^2 \sum_{(n)} f'_m T_{mn}, \qquad \Delta_n = |n| + i\pi(k_1 a)^2 J'_n(k_1 a) H^{(1)'}_n(k_1 a)$$

$$T_{mn} = (-1)^{m+1} e^{i(m-n)\xi} \begin{cases} m^{-1} V^{n-1}_{m-1}(-\cos\theta), & m \neq 0 \\ n^{-1} V^{-1}_{m-1}(-\cos\theta), & m = 0,\ n \neq 0 \\ -\ln[(1-\cos\theta)/2], & m = n = 0 \end{cases}$$

$$V^{n-1}_{m-1} = m(P_{m-1}P_n - P_{n-1}P_m)[2(m-n)]^{-1}$$

It may be shown that if the screen does not intersect the interface, then system (16) is of the Fredholm type. Its solution exists, is unique and may be approximated with any desired accuracy by means of solution of similar truncated equations. Besides, asymptotic evaluation of matrix elements as $|m| \to \infty$ shows that conditions (15) is really satisfied providing there is correct field behavior at the edges.

As for field quantities far from the origin, substitution of the series into representations like (7) yields

$$\psi^{sc}_j(\varphi) = \sum_{(n)} \mu_n J'_{-n}(k_1 a) i^n \left[\delta_{1j} e^{in\varphi} + \begin{Bmatrix} R(k_1\cos\varphi) e^{i2k_1 b\sin\varphi}, & j=1 \\ T(k_2\cos\varphi), & j=2 \end{Bmatrix} e^{-in\varphi}\right] \tag{17}$$

Integrating the squared absolute value of this function from 0 to 2π, we may calculate the value of the total scattering cross-section σ_s of the screen near the interface.

In the case of the line-current excitation, the scattered-far-field radiation pattern is to be completed by the incident-field term $\Psi^0_j(\varphi)$ which may be obtained from (A1.4). Integrating the square of this total-field function, we obtain the radiation resistance of the reflector antenna near the penetrable interface.

NUMERICAL RESULTS AND DISCUSSION

The numerical investigation has been concentrated on two scattering problems: plane wave and line-current excitation of the screen above the penetrable surface modeling short-periodic strip gratingand a similar problem of the screen near the interface between two dielectric half-spaces.

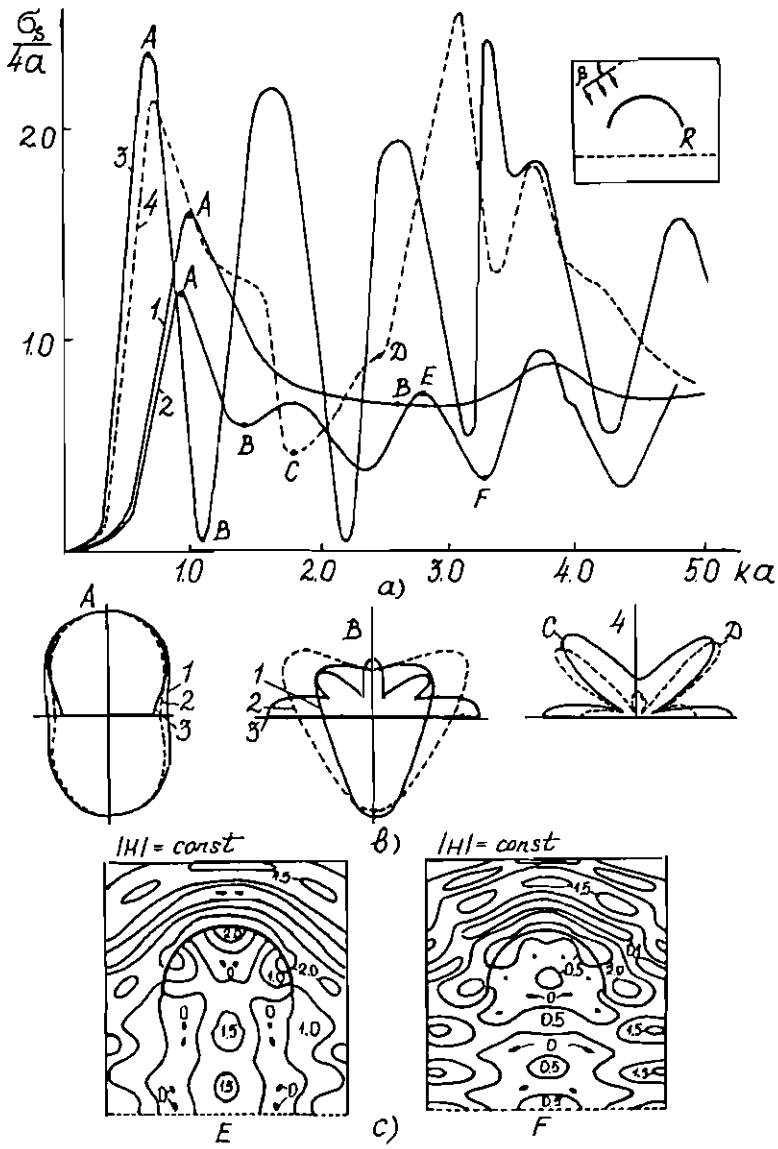

Fig.2 a) Normalized total scattering cross-section versus ka for plane wave incidence on a screen over the plane penetrable surface. $\theta = 90°$, $\xi = 270°$, $b/a = 2$,

$1.\beta = 0°$, $R = 0$; $2.\beta = 0°$, $a/l = 24$, $D/l = 0.9(R = 0.5)$

$3.\beta = 0°$, $R = 1$; $4.\beta = 45°$, $R = 1$

b) far-field scattering patterns (points from A to D at the plots of σ_s)

c) near-fields structure (E and F points at the plots of σ_s)

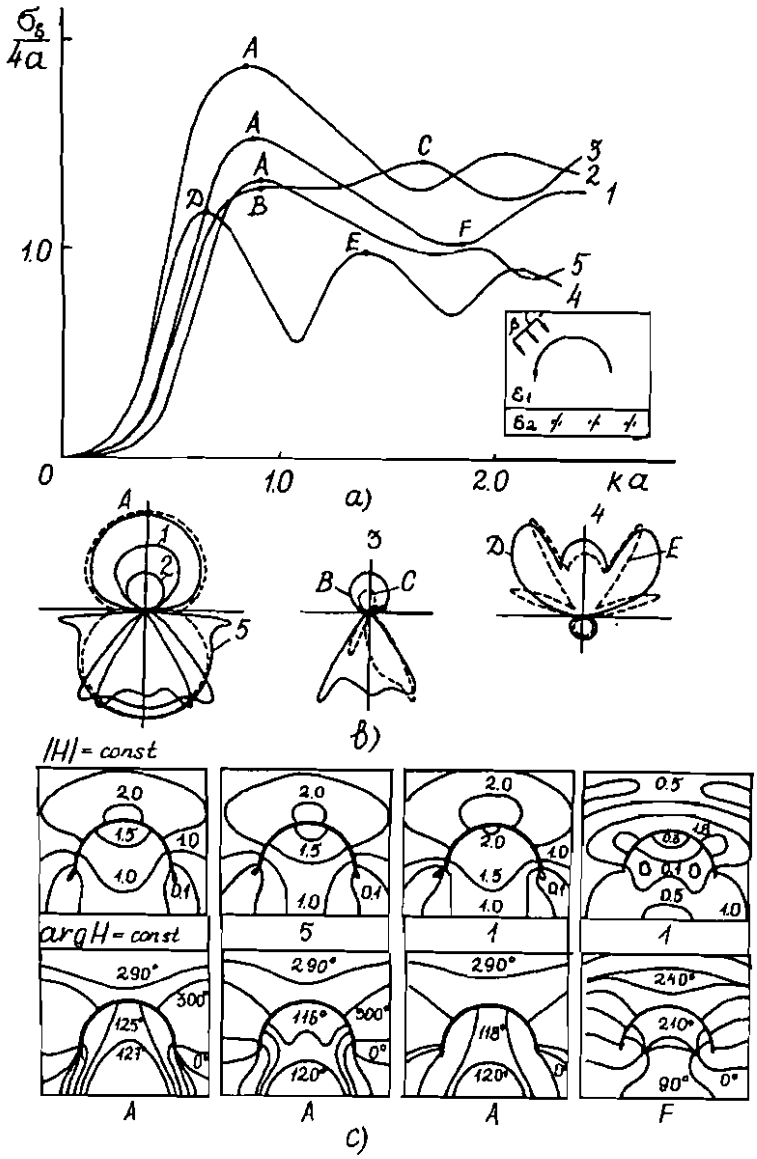

Fig.3 a) Normalized total scattering cross-section versus ka for plane wave incidence on a screen near the planar interface between two dielectric half-spaces. $\theta = 90°$, $\xi = 270°$, $b/a = 1$ 1.$\beta = 0°$, $\varepsilon_1 = 1$, $\varepsilon_2 = 2$; 2.$\beta = 0°$, $\varepsilon_1 = 1$, $\varepsilon_2 = 5$; 3.$\beta = 30°$, $\varepsilon_1 = 1$, $\varepsilon_2 = 5$; 4.$\beta = 0°$, $\varepsilon_1 = 5$, $\varepsilon_2 = 1$; 5.$\beta = 0°$, $\varepsilon_1 = 1$, $\varepsilon_2 = 1.001$

b) far-field scattering patterns (points from A to D at the plots of σ_s)

c) near-field structure (A and F points at the plots of σ_s)

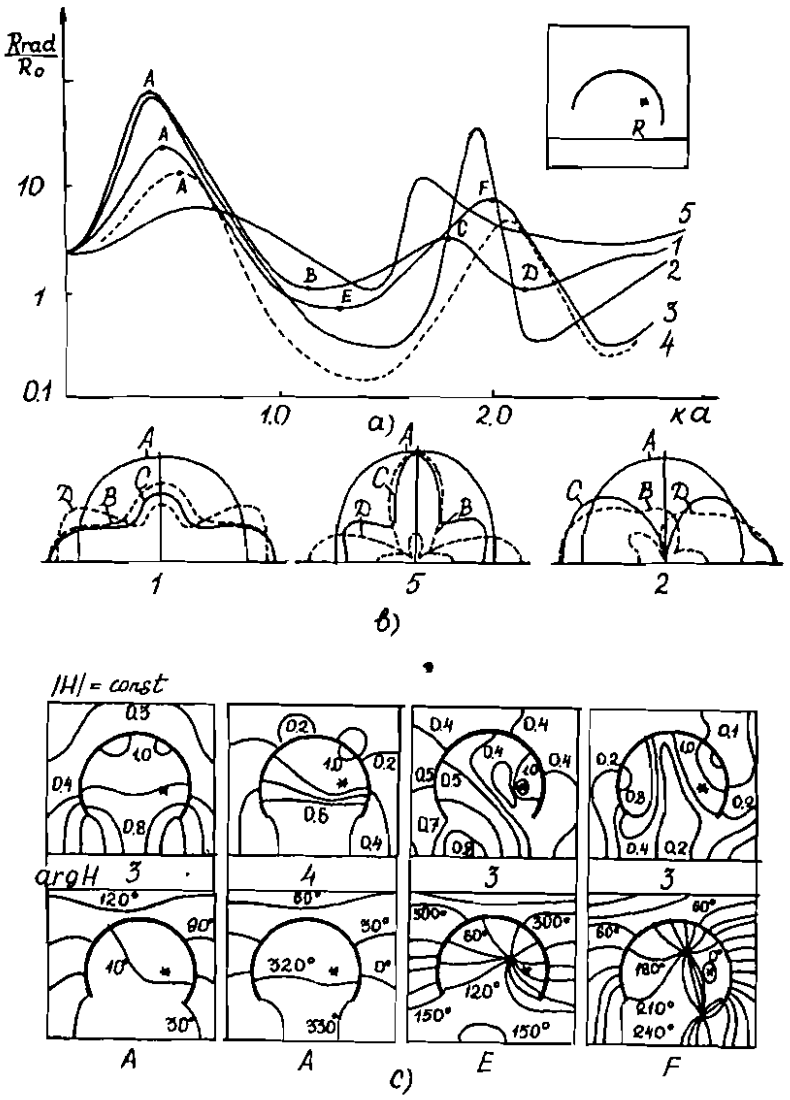

Fig.4 a) Normalized radiation resistance for line magnetic-current excitation of a screen over the plane penetrable surface, $\xi = 270^\circ$ 1.$R = 1$, $b/a = 1$, $\theta = 30^\circ$, $\varphi_0 = 90^\circ$, $r_0/a = 0.5$; 2.$R = 1$, $b/a = 1$, $\theta = 30^\circ$, $\varphi_0 = 0^\circ$, $r_0/a = 0.5$; 3.$R = 1$, $b/a = 1$, $\theta = 60^\circ$, $\varphi_0 = 0^\circ$, $r_0/a = 0.5$; 4.$a/l = 24$, $D/l = 0.9(R(0) = 0.5)$, $b/a = 1$, $\theta = 60^\circ$, $\varphi_0 = 0^\circ, \vec{r}_0/a = 0.5$

b) far-field patterns (points from A to D)

c) near-field structure (A,E,F points on the curve 3,4)

Let us first consider plane wave scattering. In Fig.2, the numerical results for the total scattering cross-section of the screen above the penetrable surface are given. A comparison with the same quantities for a free-space screen and a screen above perfectly conducting plane cases shows that there are two different sets of resonances of σ_s vs ka. The first set is associated with the screen itself (note the low-frequency resonance due to the Helmholtz mode excitation), while the second is caused by multiple reflection and interference of the fields due to the screen and its "mirror image" in the plane interface. One may easily see that if the reflectivity of the interface is decreasing, then the resonances of the first kind are shifted towards the resonant frequencies of the free-space cylinder. Naturally, the maximal values of the total cross-section are observed when both types of resonances coincide.

In the same figure both the far-field scattering patterns and the total field near-zone structures are presented which are calculated at the frequencies pointed out at the plots of σ_s.

Fig.3 demonstrates the scattered field properties of the screen near the plane boundary between two dielectric half-spaces. The scatterer is placed in the medium with a smaller dielectric constant. Two families of resonances of the same nature are observed as before, including the low-frequency Helmholtz one. In just the same manner as for other scatterers (see [1,2]), two symmetrically positioned side lobes of the pattern appear in denser media. Their position is determined by the angle of the total internal reflection, being the function of so-called contrast value $\tilde{\varepsilon} = \varepsilon_1/\varepsilon_2$. As contrast $\tilde{\varepsilon}$ increases, the angle mentioned is tending to 90°, thus both side lobes are tending to normal direction for any screen width and any plane wave angle of incidence. However, these parameters effect the widths and amplitudes of the lobes, and one of the lobes may became much greater than the other.

Let us now discuss the results of numerical simulation of reflector antenna radiation near the same boundaries as before. Figs.4 and 5 demonstrate the plots of radiation resistances R^{rad} vs ka for the screen above the grating and the dielectric interface respectively. This quantity is normalized here by the same R^0 one for free-space line-current radiation. The curves display the resonant phenomena very similar to resonances in plane-wave scattering. However, there are not only maximums in the resistance dependencies on frequency but also deep minimums.

Their nature may be explained in the way analogous to free-space scattering [4]. Exciting a natural resonance of the cylinder with a narrow slot,we obtain a powerful secondary source of radiation (or a pair of such sources, depending on the symmetry of the resonance) placed on the cylinder surface. As the frequency is varying, the phase of the secondary source is varying too, and when it becomes opposite to the phase of the primary line source, the effective far-field cancellation is observed.

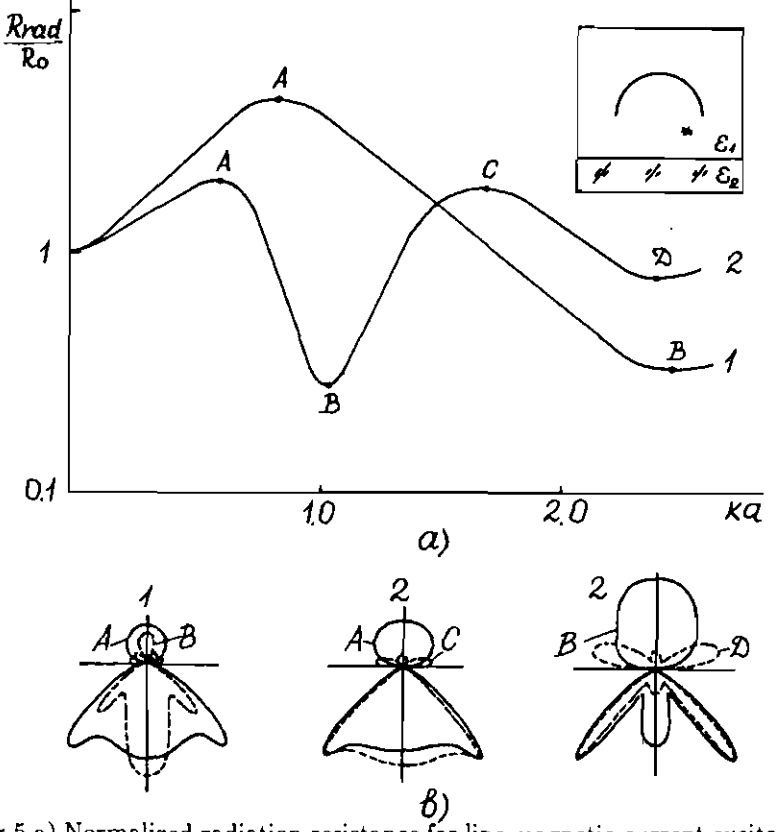

Fig.5 a) Normalized radiation resistance for line magnetic-current excitation of the screen near the planar interface between two dielectric half-spaces $\varepsilon_1 = 1$, $\varepsilon_2 = 2.28$, $\xi = 270^o$, $\theta = 90^o$, $b/a = 1.25$

$$1.\varphi_0 = 90^o,\ r_0/a = 0.5$$

$$2.\varphi_0 = 270^o,\ r_0/a = 1.2$$

b) far-field patterns at resonance points.

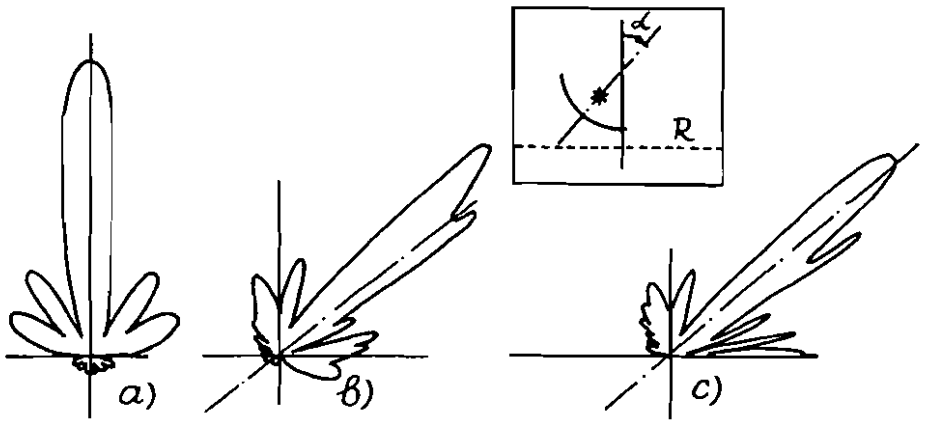

Fig.6 Far-field patterns of the reflector antenna over the plane penetrable surface. $\theta = 120°$, $ka = 20$, $r_o/a = 0.52$, $b/a = 1.25$ *a*) $a/l = 24$, $D/l = 0.93$, $\alpha = 0$ *b*) $a/l = 24$, $D/l = 0.93$, $\alpha = 50°$ *c*) $R = 1$, $\alpha = 50°$

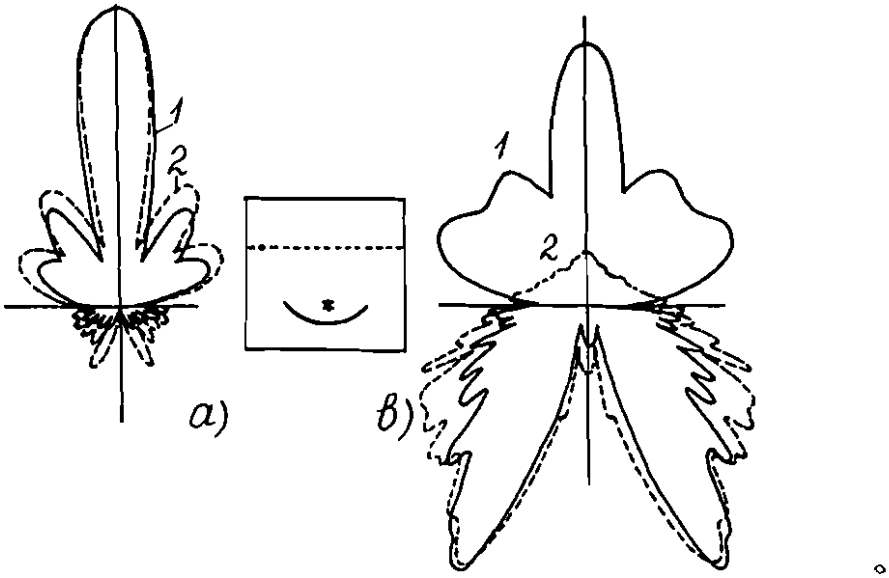

Fig.7 Far-field patterns of the reflector antenna radiating through the plane penetrable surface. $\theta = 120°$, $ka = 20$, $r_o/a = 0.52$, $b/a = 1.25$ *a*) 1. $R = 0$ 2. $a/l = 24$, $D/l = 0.85$, $(R(0) = 0.3)$ *b*) 1. $a/l = 24$, $D/l = 0.95$, $(R(0) = 0.5)$ 2. $a/l = 24$, $D/l = 0.9999$, $(R(0) = 0.7)$

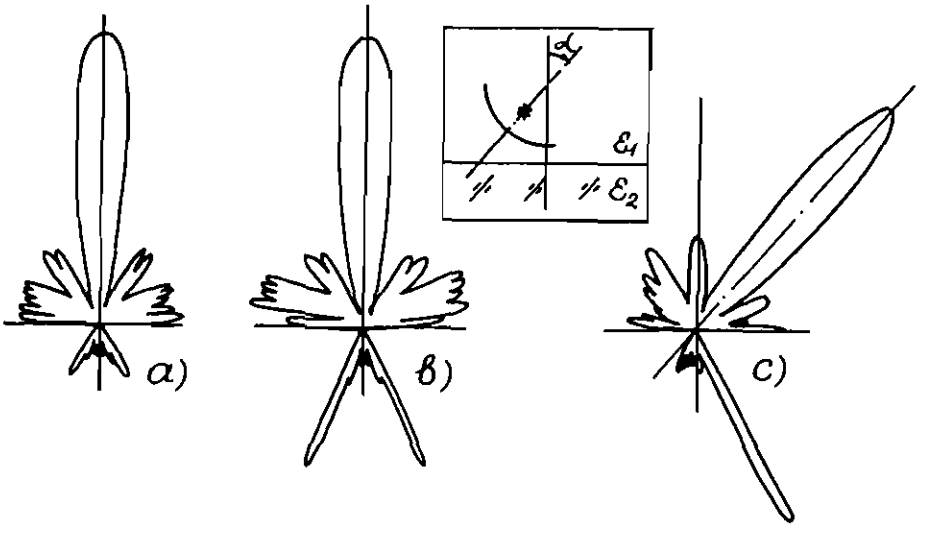

Fig.8 Far-field patterns of the reflector antenna elevated above the planar interface between two dielectric half-spaces $\theta = 120^o$, $ka = 20$, $r_o/a = 0.52$, $b/a = 1.25$, $\varepsilon_1 = 1$ *a*) $\varepsilon_2 = 4$, $\alpha = 0$ *b*) $\varepsilon_2 = 5$, $\alpha = 0$ *c*) $\varepsilon_2 = 4$, $\alpha = 40^o$

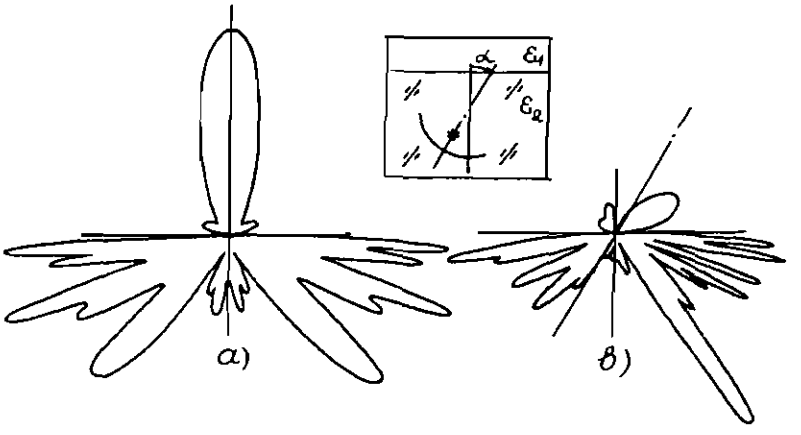

Fig.9 Far-field patterns of the "buried" reflector antenna $\theta = 120^o$, $ka = 20$, $r_o/a = 0.52$, $b/a = 1.25$, $\varepsilon_1 = 1$, $\varepsilon_2 = 4$, *a*) $\alpha = 0$, *b*)$\alpha = 30^o$

The far-field calculations enable us to determine the effect of the interface on the reflector shaping the radiation pattern. The primary line-current source has

been placed in the plane of symmetry of the screen, near the focal point.

The angular width of the screen ($\theta' = \pi - \theta = 60°$) and its dimension compared to the wavelength ($ka = 20$) were taken appropriate to simulate the parabolic reflector with good accuracy.

If the reflector antenna is located in such a way that the main lobe is directed outward, as in Fig.6, the penetrable planar interface does not affect the shape of the pattern essentially, resulting in a more complicated structure of side lobes.

In contrast to this situation, if the antenna's main lobe is radiating through the penetrable interface (here through the shortperiodic grating), then the whole pattern changes significantly and may be even damaged at all. Roughly speaking, severe damage of the far-field pattern is observed for radiation through the boundaries with the reflection coefficients greater than 0.5. The main lobe may either become less in amplitude or even be split into several separate lobes, as in Fig.7.

All the features described are typical for the reflector antenna radiation near the dielectric boundary too. Figs.8 and 9 demonstrate the radiation of "elevated" and "buried" reflector antennae respectively. There are again two characteristics side lobes caused by the effect of total internal reflection, their position is determined by the value of contrast $\tilde{\varepsilon}$ only. The higher the contrast, the greater the amplitudes of these lobes. The same effect but for only one of these lobes is observed if the reflector (and the main lobe's direction) is titled off the normal to the planar interface.

APPENDIX 1: INCIDENT FIELD

Assume the plane TE-wave is incident from the upper half-space, then

$$H_j^0(\vec{r}) = \delta_{1j} e^{ik_1(x\cos\beta - y\sin\beta)} \qquad (j = 1, 2) \tag{A1.1}$$

By using the Jacobi-Anger formula, this function can be expanded in the series over angular functions to be used in the boundary condition on the screen

$$H_j^0(\vec{r}) = \delta_{1j} \sum_{(n)} i^n J_n(k_1 r) e^{in(\varphi+\beta)} \tag{A1.2}$$

In case of the TE-line-current excitation the incident field is

$$H_j^0(\vec{r}) = \delta_{1j}(i/4) H_0^{(1)}(k_1|\vec{r} - \vec{r}_0|), \tag{A1.3}$$

where $\vec{r}_o = (r_0, \varphi_0)$ are the coordinates of the source location point. By using the addition theorem for cylindrical wave functions, we obtain the series

$$H_j^0(\vec{r}) = \delta_{1j}\frac{i}{4}\sum_{(n)}\begin{Bmatrix} J_n(k_1 r)H_n^{(1)}(k_1 r_0), & r_0 > r \\ H_n^{(1)}(k_1 r)J_n(k_1 r_0), & r > r_0 \end{Bmatrix} e^{in(\varphi-\varphi_0)} \tag{A1.4}$$

convenient for substitution into the boundary condition equation.

One may easily see that the right-hand-part expansion coefficients for plane wave excitation are

$$f_n' = i^n J_n'(k_1 a)e^{in\beta} \tag{A1.5}$$

For line-current excitation the analogous coefficients are

$$f_n' = \frac{i}{4}J_n'(k_1 a)H_n^{(1)}(k_1 r_0)e^{-in\varphi_0}, \tag{A1.6}$$

if the source is located inside the circle of the screen's radius. These are the quantities used in numerical simulations.

APPENDIX 2: DIELECTRIC INTERFACE AND SHORTPERIODIC STRIP GRATING

Considering plane wave reflection and transmission through the flat interface between two dielectric half-spaces, one may derive the following expressions

$$R(h) = \frac{(1-h^2k^2)^{1/2} - (\tilde{\varepsilon} - \tilde{\varepsilon}^2 h^2/k^2)^{1/2}}{(1-h^2k^2)^{1/2} + (\tilde{\varepsilon} - \tilde{\varepsilon}^2 h^2/k^2)^{1/2}} \tag{A2.1}$$

$$T(h) = \frac{2(1-h^2k^2)^{1/2}}{(1-h^2k^2)^{1/2} + (\tilde{\varepsilon} - \tilde{\varepsilon}^2 h^2/k^2)^{1/2}} \tag{A2.2}$$

Taking $h = k_1 \cos\alpha$, we can obtain from (A2.1), (A2.2) the well- known formulae for the reflection and transmission coefficients of the TE-polarized plane wave incident at the angle α : $\cos\alpha = h/k_1$.

As for the periodic gratings, the full-wave solution operates in term of an infinite number of grating space harmonics. Thus, the Fourier transforms of the Green's function above and below the grating are presented by series

$$\tilde{G}_{1j}^{sc} = \frac{1}{g}e^{igy'-ihx'}\sum_{(q)}\begin{Bmatrix} a_q(h), & j=1 \\ b_q(h), & j=2 \end{Bmatrix} e^{ig_q|y+b|+ikx_q\kappa^{-1}}, \tag{A2.3}$$

where $\kappa = kl/2\pi$, $h_q = h + qk/\kappa$, $g_q = (k^2 - h_q^2)^{1/2}, q = 0, \pm 1, \ldots$, $\varepsilon_1 = \varepsilon_2 = 1$ (free-space surrounding), l is the period, $\vec{r}' \in S_1$, $\vec{r} \in S_j$, $(j = 1, 2)$.

Procedure of seeking for the gratings modes harmonics $a_q(h)$ and $b_q(h)$ varies greatly for different types of gratings [7]. E.g., for the grating of planar perfectly conducting strips, it exploits the Riemann-Hilbert Problem technique, resulting in the infinite matrix equations of the Fredholm type [8].

Nevertheless, if the grating is shortperiodic, it is possible to neglect all the modes except the zero one because they are of the order of $O(\kappa^2)$. Then for planar grating of perfectly conducting strips, the so-called Lamb approximation is valid [7]. Denoting $a_0(h) = R(h)$ and $b_0(h) = T(h)$, we can use explicit formulae

$$R(h) = \frac{i\kappa Q(1 - h^2/k^2)^{1/2}}{1 - i\kappa Q(1 - h^2/k^2)^{1/2}} \qquad T(h) = \frac{1}{1 - i\kappa Q(1 - h^2/k^2)^{1/2}} \qquad \text{(A2.4)}$$

where $Q = -2\ln\cos(\pi D/l)$, D is the strip width.

REFERENCES

1. X.-B. Xu, C.M.Butler, Current induced by TE excitation on a conducting cylinder located near the planar interface between two semi-infinite half-spaces. IEEE Trans.Antennas Propagat., vol.AP-34, no.7, pp.880-890, July 1986.
2. X.-B. Xu, C.M.Butler, Scattering of TE excitation by coupled and partially buried cylinders at the interface between two media. IEEE Trans.Antennas Propagat., AP-35, no.5, pp.529-538, May 1987.
3. E.I. Veliev, V.V. Veremey, V.P. Shestopalov, The principal characteristics of small antennae formed by unclosed cylindrical screens. Radiophysics and Quantum Electronics, 1984, vol.27.
4. E.I.Veliev, V.V.Veremey, A.I.Nosich and V.P.Shestopalov, Trapping effect in excitation of an unclosed screen by a localized source. Radiophysics and Quantum Electronics, 1982, vol.25, no. 4.
5. A.I.Nosich, Radiation conditions for open waveguides. SovietPhysics-Doklady, 1987, vol.32, no.9, pp.720-722.
6. V.P.Shestopalov, Dual series equations in the modern theory of diffraction, Naukova dumka Press, Kiev, 1983 (in Russian).

7. V.P.Shestopalov, L.N.Litvinenko, S.A.Masalov and V.G.Sologub, Diffraction of waves by gratings, Vistcha shkola Publ., Kharkov, 1973 (in Russian).
8. N.V.Veremey, V.V.Veremey, Excitation of an cylindrical reflector in the vicinity of the perfectly conducting or semi-transparent planar surface. Sci.Report no.5635-B89, Izv.VUZov Radiophisika, 1989.